Membrane-based receiver/transmitter for reconfigurable optical wireless beam-steering systems

Membrane-based receiver/transmitter for reconfigurable optical wireless beam-steering systems

Yuqing Jiao, *Member, IEEE*, Zizheng Cao, *Member, IEEE*, Longfei Shen,
Jos van der Tol and Ton Koonen, *Fellow, IEEE*

***Abstract*—In this paper a novel integrated optical wireless receiver/transmitter is presented. The device is realized on an InP membrane platform where active and passive components are integrated monolithically. It can be reconfigured to either receiver mode or transmitter mode, by simple control on the operation mode of a photodetector (short SOA). Demonstration of the receiver mode in an indoor optical wireless system has shown 17.4 Gbps OFDM signal transmission, illustrating the potential of this concept.**

***Index Terms*— Photonic integrated circuit (PIC), membrane, indium phosphide (InP), photodetector, grating, optical wireless communication (OWC).**

I. Introduction

THE abundant proliferation of mobile terminals is causing radio spectrum congestion and mutual interference, which seriously limit the wireless connectivity. The free space optical wireless communication (OWC) is an alternative option with the advantage of providing a huge unlicensed bandwidth. OWC using light emitting diode (LED) based visible light has however a very limited bandwidth (only a few tens of MHz), whereas with visible lasers the optical transmitted power is limited by eye safety regulations. Optical wireless communication can better use infrared wavelengths, in particular with regard to eye safety levels. According to the ANZI Z-136 and IEC 60825-1 eye safety standards, the lasers at IR wavelength (1400nm-4000nm) are allowed to emit > 200 times more optical power as compared to visible wavelengths. Steering of a highly concentrated optical beam is of particular interest in in-door applications, providing secure and high capacity link [1]. 2D optical beam steering has been demonstrated recently by various techniques, for instance, wavelength-assisted pencil beams [2] and compact grating array [3]. On the receiver side, in order to receive more optical power, a large area of light acceptance is required. A solution may be to use a photodiode (PD) array to increase the optical aperture for better reception. Imaging diversity may be deployed, where an array of light sources is mapped to an array of detectors. As shown in [4], a 7-channel diversity receiver equipped with a hexagonal metal–semiconductor–metal (MSM) InGaAs photodetector array achieves a data rate of 5 Gb/s using multiple-input and multiple-output (MIMO) techniques. Alternatively, an angle diversity transceiver may be deployed, where the sources emit at different angles and the receiver has multiple detectors looking into these different angles [5]. To allow the independent optimization of electrical and optical features of the optical receiver, we proposed a cascaded acceptance optical receiver (CAO-Rx) in [6]. The present paper provides an extension of our research with detailed investigation on the CAO-Rx. The paper is organized as follows. Section II investigates: the operation principle for a reconfigurable CAO-Rx. Detailed characterization of the integrated CAO-Rx is provided in Section III. Section IV describes the 17 Gbps indoor optical wireless system based on the integrated CAO-Rx. The experimental results are then discussed in Section V. Finally we conclude the paper.

II. Reconfigurable Concept

The schematic illustration of the reconfigurable wireless receiver is given in Fig. 1. The concept is mainly composed of two parts: an optical antenna and an optical translator. An optical coupler serves as the optical antenna. It couples the free-space optical beams and the guided modes in the waveguide. A p-i-n diode serves as the optical translator. It can either translate the input optical signal into electrical signal, or translate the input signal unchanged to its output.

In the receiver mode (Fig. 1(a)), the p-i-n diode is reverse biased to act as a photodetector (PD). The reverse bias can ensure a high responsivity and a high speed operation of the PD. The PD absorbs the light which is coupled into the waveguide through the optical coupler, and converts it into electrical current. In the emitter mode (Fig. 1(b)), the p-i-n diode acts as a transparent gate. The diode will be transparent to the optical signal propagating though it, when the injected

This work was supported by the ERC Advanced Grant BROWSE and the ERC Advanced Grant NOLIMITS. The concept of cascaded aperture optical receiver for optical beam steering is created by Z. Cao. Y. Jiao extends this idea with reconfigurable operation for transmitter and receiver.

Y. Jiao, L. Shen and J.v.d. Tol are with the Photonic Integration (PhI) group, Institute for Photonic Integration, Eindhoven University of Technology, PO Box 513, 5600MB Eindhoven, The Netherlands. (e-mail: y.jiao@tue.nl).

Z. Cao and T. Koonen are with the Electro-Optical Communications (ECO) group, Institute for Photonic Integration, Eindhoven University of Technology, PO Box 513, 5600MB Eindhoven, The Netherlands. (e-mail: z.cao@tue.nl). The corresponding author is Z. Cao (z.cao@tue.nl).

current at forward bias reaches the transparency level. Therefore the optical signal from the source can be transported to the optical coupler without extra loss, or even with extra gain.

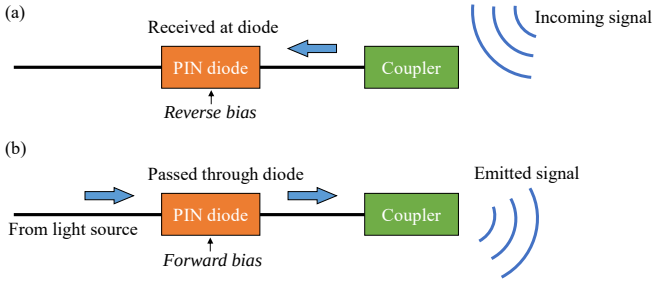

Fig. 1. Schematic illustration of the reconfigurable optical wireless receiver: (a) receiver mode; (b) emitter mode.

The most valuable advantage of this scheme is the sharing of the circuits for the transmitter and receiver modes. The p-i-n diode, the optical coupler as well as the access waveguides can all be used in both operation modes. Therefore the device footprint and the fabrication complexity can be significantly reduced. This is very useful in the context of large-scale optical antenna arrays. As can be seen in Fig. 1, the core components of this scheme are the diode and the coupler. The key idea is to use a short SOA section as an efficient photodetector. For transmitter mode an on-chip laser should be integrated. In this fabricated chip, the laser can only be operated at pulsed mode with low output power, due to fabrication issues [7]. In this paper we focus on the receiver configuration, where the key roles of the diode and the coupler are demonstrated.

III. Chip Fabrication

The device is realized in the indium phosphide on silicon (IMOS) platform [8], where high-confinement waveguides, surface gratings, SOAs and lasers are integrated monolithically on a single thin membrane [7, 9], as illustrated in Fig. 2. The thin membrane consist of both active and passive components, defined with different etch depths.

The entire membrane is bonded onto a silicon wafer using benzocyclobutene (BCB) polymer [10]. The thickness of the optical buffer layer (1850 nm in total, combining SiO_2 and BCB layers) is optimized to avoid light leakage into the substrate and to obtain efficient coupling between grating couplers and optical fibers. The III-V membrane layerstack consists of two vertically stacked waveguide cores, forming a twin-guide structure. The two waveguide cores are coupled with short adiabatic tapers. The lower intrinsic InP core (300 nm thick) acts as the passive waveguiding layer. With a width of 400 nm, the passive waveguide can support both fundamental tranverse electric (TE) and transverse magnetic (TM) modes, and provides high optical confinement, low propagation loss [11, 12] and sharp bending [13].

The 250 nm bulk intrinsic InGaAsP quaternary layer is used as the active core, located on top of the passive core. Its bandgap corresponds to the wavelength of 1.58 μm. On top of it are p-doped contact layers with total thickness of 400 nm. The n-doped contact layers are placed in between the active and passive cores and have a total thickness of 100 nm. Metal contacts for the amplifiers and detectors are defined on top of the p- and n-doped contact layers using Ti/Pt/Au and Ni/Ge/Au metal stacks, respectively.

The fabrication of the membrane photonic chip starts with the amplifier/detector sections. The ridge structures of the amplifier/detector are defined with electron-beam lithography (EBL) and reactive ion etching (RIE). The n-contact region is then defined and protected. To form the passive waveguides and surface gratings, two EBL and RIE cycles are used. Finally the p- and n-metals are deposited using electron-beam evaporation. The more detailed fabrication process can be found in [7, 14].

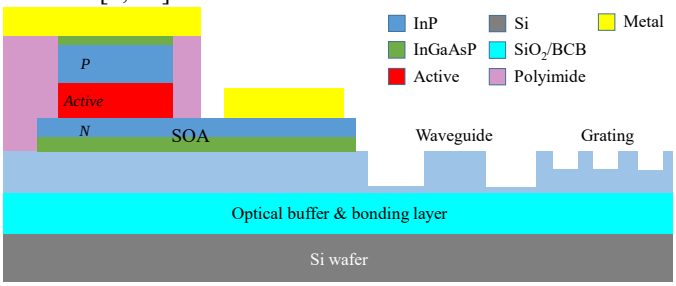

Fig. 2. Schematic diagram of the IMOS platform.

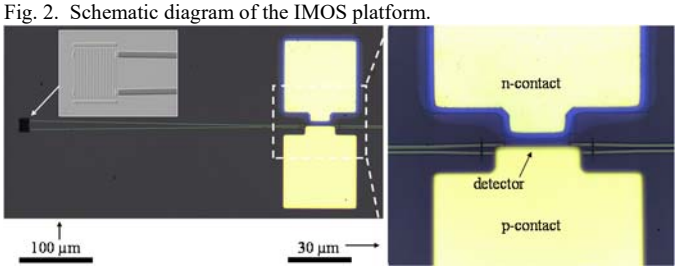

Fig. 3. Microscope picture of the fabricated receiver device. Left inset: SEM picture of the surface grating; right inset: enlarged picture of the detector.

For a demonstration as a receiver, a circuit consisting of a surface grating and a PD, as shown in Fig. 3, is used.

The surface grating is shallowly etched into the 300 nm thick passive waveguide. The etch depth is 120 nm. The grating has 20 periods with a period of 660 nm and a 50 % fill factor. It has a central wavelength of 1550 nm at an incident angle of 10°. The grating is designed to couple light between fundamental TE mode in the waveguide and a free-space Gaussian beam with a 5 μm waist. The grating coupler has a mode divergence similar to the guided mode output from a

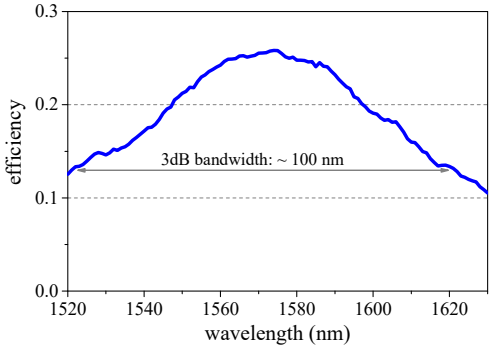

Fig. 4. Measured spectral efficiency of a reference surface grating fabricated together with the membrane optical wireless receivers.

single-mode optical fiber, because the emitted mode in the grating is similar to the mode in the fiber. We experimentally measured the field of view (FOV) of the grating to be about 7.5°. Beam-steering is still feasible using such gratings with relatively large footprint and small FOV [15, 16]. Figure 4 shows the measured spectral efficiency of a reference grating, which is identically designed and fabricated on the same chip as the receiver. The peak efficiency of 25 % and the 3-dB bandwidth of 100 nm are typical for such dielectric gratings. The collected light is transported to the input of the detector through an adiabatic taper structure and a 100 µm long single-mode waveguide.

A reverse-biased short SOA section with a length of 40 µm (30 µm SOA + 2 × 5 µm tapers) is used as the PD. The PD thus has the identical structure as the longer SOAs used in the membrane lasers [7], indicating the potential for recon-figurability as a transparent gate in the transmitter mode. The static performance of the detector is shown in Fig. 5. The detector maintains a low dark current (below 45 nA) for a reverse bias range of 0 to 3 V (Fig. 5(a)). The responsivity of the device (Fig. 5(b)) can reach up to 0.89 A/W at 3 V reverse bias, at a wavelength of 1575 nm. The responsivity at 1550 nm wavelength is 0.75 A/W. These responsivity values are corrected for the 6 dB insertion loss from the surface grating. The 3 dB bandwidth as well as the spectral shape of the responsivity curves is dominated by the spectral response of the surface grating.

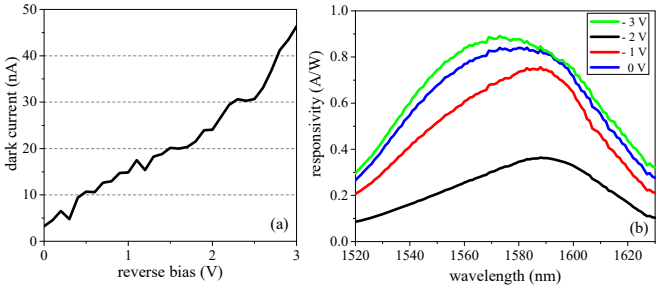

Fig. 5. (a) Dark current of the PD as a function of reverse bias voltages. (b) Spectral response of the PD at 3 V reverse bias.

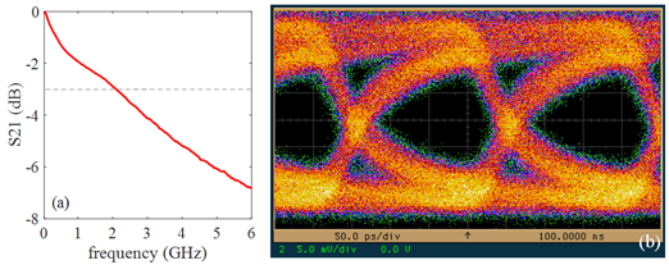

Fig. 6. (a) Small signal frequency response of the detector. (b) Eye diagram of the detector at 5 Gb/s data rate.

The dynamic behavior of the detector is also characterized. The small signal electrical bandwidth is measured with an Agilent network analyzer. The measured result indicates a 3dB bandwidth of 2 GHz (see Fig. 6(a)). This is mainly limited by a fabrication issue in the metal contact, which can be improved with optimized fabrication. Moreover, this bandwidth does not hinder the receiver demonstration, since any improvements on the detector will not influence the other components in the receiver. The eye diagram of the photocurrent, at an on-off keying (OOK) data rate of 5 Gb/s, is shown in Fig. 6(b). The input optical power before entering the grating coupler is 5.1 dBm. No electrical amplification is used. As can be seen a clear opening of the eye at 5 Gb/s is obtained.

IV. Indoor Optical Wireless System

Figure 7 shows the experimental setup for 17.4 Gbps optical wireless transmission based on the CAO-Rx. A 10-dBm optical carrier is generated from a commercial semiconductor laser diode. The orthogonal frequency division multiplexing (OFDM) waveform, consisting of 256 subcarriers within the baseband bandwidth of 4.68 GHz, is uploaded in the arbitrary waveform generator (AWG, Tektronix 7122B @ 12 GSa/s). From the 256 subcarriers of the OFDM waveform, numbers 192, 8, and 56 are designated to data, pilots and high frequency guard-band (HFGB), respectively. Note that the HFGB is used to suppress the out-of-band spectrum of the OFDM signal. The subcarriers of the OFDM signal are arranged to satisfy the Hermitian symmetry for the real-valued IFFT output. The period of an OFDM symbol is 22 ns, and thus the symbol rate for each subcarrier is 45.4 MSymbol/s. 16-QAM is employed for the data subcarrier modulation. The cyclic prefix is 1/32 of an OFDM period, which corresponds to 8 samples in every OFDM symbol. One training symbol is inserted in front of 320 data OFDM symbols for the symbol synchronization and channel estimation. The OFDM signal from the output of the AWG with 1 V peak-peak amplitude is amplified by means of a 12 GHz broadband amplifier (SHF100APP). The amplified signal is then modulated on the optical carrier via a 10 GHz commercial Mach-Zehnder modulator (MZM) biased at the linear region of the power transfer curve. The insertion loss of the MZM is then compensated by an EDFA, providing the output optical power of about 12 dBm. The optical power is then attenuated before being launched to the input end of the cleaved fiber. The lightwave from the output end of the fiber is shone onto the CAO-Rx after a free space separation of about 800 µm. The cleave fiber is used to provide the proof of concept, since the CAO-Rx is still in packaging phase before being used for wide angle FSO link. The cleaved fiber is with 10° angle offset of the SG perpendicular. The experimental setup is shown in Fig. 7. The lightwave signal leaves from the cleaved fiber will propagate in free space before it incidents on the surface grating. Since the engaged surface grating is polarization dependent, a polarization controller is used to tune the lightwave polarization for an optimized acceptance. An Eigen Light 410 is used as an optical attenuator and in-line optical power monitor. The electrical signal at the PD output is collected with a high-speed ground-signal (GS) probe matching the p- and n-metal pads. The 3V DC reverse bias is applied to the PD. The received OFDM signal is then separated by the DC via a bias-T, which is then amplified by a 12 GHz broadband amplifier (SHF100APP) with bias voltage of 7.94 V. The resulting signal is then sampled and stored by a commercial real time oscilloscope (Tektronix DPO70000) for offline processing.

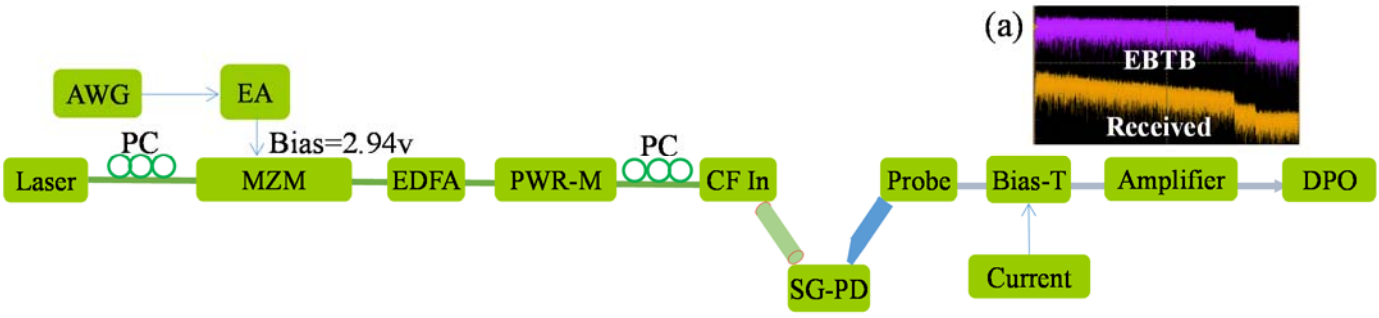

Fig. 7. Experimental setup of optical wireless data transfer based on the fabricated CAO-Rx. (a) RF spectrum of OFDM signal at EBTB and received at CAO-Rx

V. Results and Discussion

The frequency spectrum of the received OFDM signal is compared with the EBTB signal as depicted in Fig. 7(a). High frequency fading is observed, which mainly comes from the limited bandwidth of the MZM, the electrical amplifiers, the cables and the CAO-Rx itself. Such high frequency fading does not introduce a severe power penalty at high frequency subcarriers, hence the data transmission is guaranteed.

The photocurrent from the PD and the bit error rate (BER) versus the input optical power at 17.4 Gbps are shown in Fig. 8, for three different laser wavelengths (1540, 1550 and 1560 nm). The PD has different responsivities at those wavelengths, as can be seen from Fig. 5(b). This results in different photocurrents generated in the PD. Thelonger wavelength (1560 nm) is closer to the peak responsivity at 1575 nm. It thus generates a higher photocurrent, as shown in Fig. 8(a). The bit error rate (BER) of the transmitted signal is therefore wavelength dependent (Fig. 8(b)). As the optical wavelength approaches 1575 nm, the BER reduces significantly. At 1560 nm wavelength, a BER of 3.8×10^{-3} can be achieved at an ROP of about -3.75 dBm, which is below the common forward error correction (FEC) limit. Moreover, the BER difference between different wavelengths gets smaller as the optical power increases. The sensitivity of the CAO-Rx will further be improved by more accurate grating-waveguide coupling in the packaging phase.

The constellations for an ROP of -1.5 dBm at 1560 nm, and for an ROP of -4.5 dBm at 1540 nm are shown in Fig. 9(a) and (b), respectively. Fig. 9(b) shows a blurrier constellation with a higher BER, which is due to the off-center wavelength and the lower ROP level. With the same settings as for Fig. 9(a), the bit error distribution versus subcarrier index (frequency axis) and OFDM frame number (time axis) are shown in Fig. 9(c) and (c), respectively. It is obvious that the bit errors dramatically increase at higher frequency. However, the bit errors along time axis show a random distribution. This could be due to a slight instability in the measurement setup.

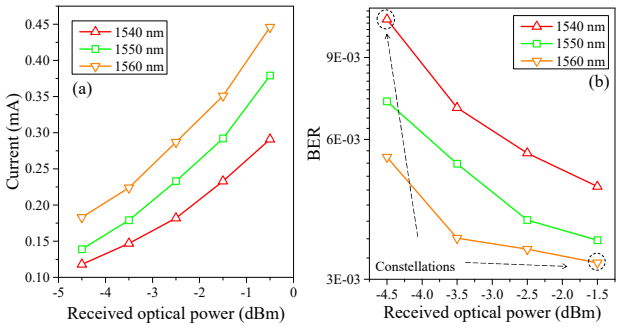

Fig. 8. (a) Photocurrent from the PD, and (b) BER as a function of received optical power for three different wavelengths.

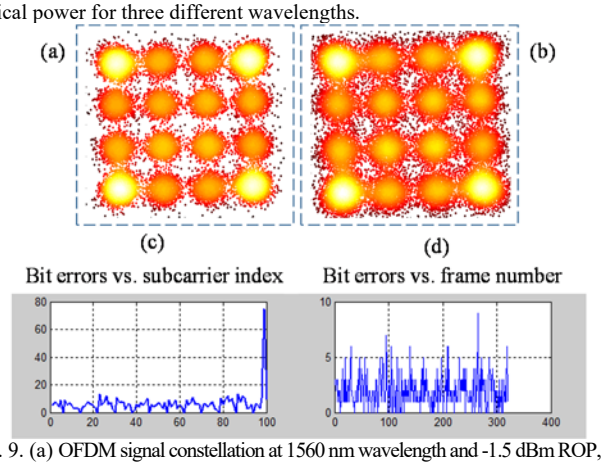

Fig. 9. (a) OFDM signal constellation at 1560 nm wavelength and -1.5 dBm ROP, (b) OFDM signal constellation at 1540 nm wavelength and -4.5 dBm ROP. Bit error distribution versus (c) subcarrier index and (d) OFDM frame.

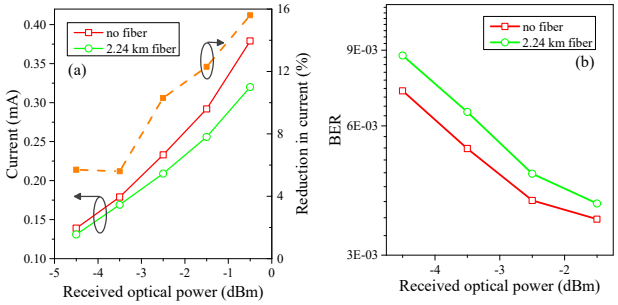

Fig. 10. (a) Photocurrent from the PD, and (b) BER as a function of input optical power, with and without the 2.24 km long optical fiber. The wavelength is 1550 nm.

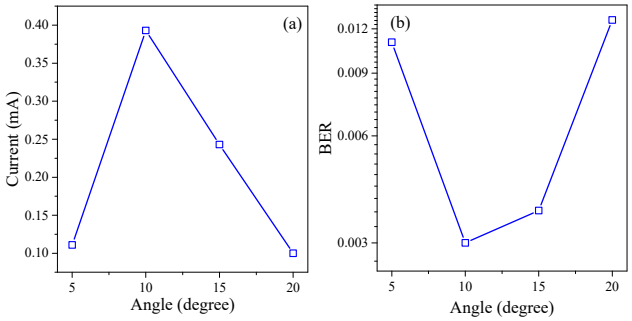

Fig. 11. (a) Photocurrent from the PD, and (b) BER as a function of beam incident angle, at optical power of 12.5 dBm and wavelength of 1560 nm.

In an actual in-door optical wireless architecture, there will be optical fibers employed to deliver the optical signal into each room at low cost [17]. To test this scenario a 2.24 km long fiber was inserted between the EDFA and the cleaved fiber tip (see Fig. 7. The insertion loss of this fiber is 1.3 dB.

This results in a reduction of the photocurrent from the PD, as shown in Fig. 10(a). However, it can also be seen that the fraction of the reduced current increases as the ROP increases. This is mainly due to the nonlinear responsivity in the p-i-n based PDs. The consequence of the extra loss in the 2.24 km long fiber is an increase in BER, as shown in Fig. 10(b). The power penalty induced by the increased BER also shows a nonlinear trend with different ROP levels. A power penalty of 1 dB is observed at a relatively high ROP level (around -2 dBm). The penalty reduces to approximately 0.6 dB at a relatively low ROP levels (< -3 dBm). This is directly correlated to the power-dependent responsivity of the PD.

The performance of the device at different beam incident angles is also evaluated. The change of the incident beam angle is realized by changing the tilt angle of the optical fiber which launches the free-space beam. Fig. 11(a) shows the change of photocurrent received at the PD as the beam angle changes from 5° to 20°. The result clearly shows the highest photocurrent at the optimized 10° angle. As the incident angle deviates from 10°, the efficiency of the grating coupler drops, which directly influences the current generated in the PD. The angle dependency gives a direct impact on the BER of the data transmission, as shown in Fig. 11(b). The BER deteriorates at non-optimal angles. From the figure it can be seen that the angular tolerance of the current grating coupler is about 6°, when considering the FEC limit of 3.5×10^{-3}. This grating was originally optimized for fiber coupling, with shallow pitches and a relatively large footprint in order to match the fiber mode. The angle coverage can be significantly enhanced by using a grating design with deeply etched pitches [18].

VI. Conclusions

The concept of an integrated CAO-Rx for free-space optical wireless communication is proposed in this paper. The receiver is novel in terms of its reconfigurability. It can be switched between receiver mode and transmitter mode by simply switching the operation condition of the photodetector. The receiver has been fabricated in an active-passive InP membrane platform and applied in an indoor OWC system. An OFDM optical wireless data transmission of 17.4 Gbps, and a BER less than 3.8×10^{-3} have been achieved at a received optical power of -3.75 dBm. Since the optical efficiency and electrical bandwidth can be optimized independently, the CAO-Rx concept can inherently provide a flexible solution for future optical wireless systems, with a high optical efficiency and a large electrical bandwidth.

References

[1] Z. Cao, Q. Ma, A. B. Smolders, Y. Jiao, M. J. Wale, J. Oh, H. Wu, and A. M. J. Koonen, "Advanced Integration Techniques on Broadband Millimeter-wave Beam Steering for 5G and Beyond," *IEEE Journal of Quantum Electronics,* vol. 52, pp. 1-20, 2016.

[2] T. Koonen, J. Oh, K. Mekonnen, Z. Cao, and E. Tangdiongga, "Ultra-High Capacity Indoor Optical Wireless Communication Using 2D-Steered Pencil Beams," *Journal of Lightwave Technology,* vol. 34, pp. 4802-4809, 2016.

[3] J. Sun, E. Timurdogan, A. Yaacobi, E. S. Hosseini, and M. R. Watts, "Large-scale nanophotonic phased array," *Nature,* vol. 493, pp. 195-199, 2013.

[4] J. Zeng, V. Joyner, L. Jun, D. Shengling, and H. Zhaoran, "A 5Gb/s 7-channel current-mode imaging receiver front-end for free-space optical MIMO," in *Circuits and Systems, 2009. MWSCAS '09. 52nd IEEE International Midwest Symposium on*, 2009, pp. 148-151.

[5] D. O'Brien, R. Turnbull, M. Hoa Le, G. Faulkner, O. Bouchet, P. Porcon, M. El Tabach, E. Gueutier, M. Wolf, L. Grobe, and L. Jianhui, "High-Speed Optical Wireless Demonstrators: Conclusions and Future Directions," *Lightwave Technology, Journal of,* vol. 30, pp. 2181-2187, 2012.

[6] Z. Cao, Y. Jiao, L. Shen, F. Yan, A. Khalid, T. LI, X. Zhao, N. Tessema, J. Oh, and T. Koonen, "Optical wireless data transfer enabled by a cascaded acceptance optical receiver fabricated in an InP membrane platform," in *Optical Fiber Communication Conference*, 2016, p. M2B. 3.

[7] Y. Jiao, D. Heiss, L. Shen, S. Bhat, M. Smit, and J. van der Tol, "First Demonstration of an Electrically Pumped Laser in the InP Membrane on Silicon Platform," in *Advanced Photonics 2015*, Boston, Massachusetts, 2015, p. IM4B.3.

[8] J. van der Tol, J. Pello, S. Bhat, Y. Jiao, D. Heiss, G. Roelkens, H. Ambrosius, and M. Smit, "Photonic integration in indium-phosphide membranes on silicon (IMOS)," in *Proc. SPIE 8988, Integrated Optics: Devices, Materials, and Technologies XVIII*, 2014, pp. 89880M-89880M-17.

[9] K. A. Williams, E. A. J. M. Bente, D. Heiss, Y. Jiao, K. Ławniczuk, X. J. M. Leijtens, J. J. G. M. van der Tol, and M. K. Smit, "InP photonic circuits using generic integration [Invited]," *Photonics Research,* vol. 3, pp. B60-B68, 2015.

[10] S. Keyvaninia, M. Muneeb, S. Stankovi, P. J. Van Veldhoven, D. Van Thourhout, and G. Roelkens, "Ultra-thin DVS-BCB adhesive bonding of III-V wafers, dies and multiple dies to a patterned silicon-on-insulator substrate," *Opt. Mater. Express,* vol. 3, pp. 35-46, 2013.

[11] Y. Jiao, J. Pello, A. M. Mejia, L. Shen, B. Smalbrugge, E. J. Geluk, M. Smit, and J. van der Tol, "Fullerene-assisted electron-beam lithography for pattern improvement and loss reduction in InP membrane waveguide devices," *Optics Letters,* vol. 39, pp. 1645-1648, 2014.

[12] Y. Jiao, T. de Vries, R.-S. Unger, L. Shen, H. Ambrosius, C. Radu, M. Arens, M. Smit, and J. van der Tol, "Vertical and Smooth Single-Step Reactive Ion Etching Process for InP Membrane Waveguides," *Journal of The Electrochemical Society,* vol. 162, pp. E90-E95, 2015.

[13] Y. Jiao, J. Liu, A. M. Mejia, L. Shen, and J. v. d. Tol, "Ultra-Sharp and Highly Tolerant Waveguide Bends for InP Photonic Membrane Circuits," *IEEE Photonics Technology Letters,* vol. 28, pp. 1637-1640, 2016.

[14] Y. Jiao, D. Heiss, L. Shen, S. P. Bhat, M. K. Smit, and J. J. G. M. v. d. Tol, "Design and Fabrication Technology for a Twin-Guide SOA Concept on InP Membranes," in *Proceedings of the 17th European Conference on Integrated Optics and Technical Exhibitionan, 19th Microoptics Conference (ECIO-MOC)*, 2014.

[15] J. K. Doylend, M. J. R. Heck, J. T. Bovington, J. D. Peters, L. A. Coldren, and J. E. Bowers, "Two-dimensional free-space beam steering

with an optical phased array on silicon-on-insulator," *Optics Express,* vol. 19, pp. 21595-21604, 2011.
[16] W. Guo, P. R. A. Binetti, C. Althouse, M. L. Masanovic, H. P. M. M. Ambrosius, L. A. Johansson, and L. A. Coldren, "Two-Dimensional Optical Beam Steering With InP-Based Photonic Integrated Circuits," *IEEE Journal of Selected Topics in Quantum Electronics,* vol. 19, pp. 6100212-6100212, 2013.
[17] T. Koonen and Z. Cao, "Optically controlled 2D radio beam steering system," in *2014 International Topical Meeting on Microwave Photonics (MWP) and the 2014 9th Asia-Pacific Microwave Photonics Conference (APMP)*, 2014, pp. 389-391.
[18] S. Jie, E. Timurdogan, A. Yaacobi, S. Zhan, E. S. Hosseini, D. B. Cole, and M. R. Watts, "Large-Scale Silicon Photonic Circuits for Optical Phased Arrays," *Selected Topics in Quantum Electronics, IEEE Journal of,* vol. 20, pp. 264-278, 2014.

Yuqing Jiao was born in Hangzhou, China. He obtained PhD degrees from both Eindhoven University of Technology, the Netherlands, and Zhejiang University in China in 2013. Since then he continued his research at Eindhoven University of Technology. Since 2016 he is appointed as an assistant professor at the Institute of Photonic Integration (IPI, former COBRA Research Institute) of the Eindhoven University of Technology. His research topic is focused on a novel III-V based nanophotonic platform. He is focusing on ultrafast and strong light-matter interactions in sub-micron optical confinement. Applications span from optical interconnects, ultrafast photonic devices, to optical beam steering and optical sensing. He has strong background and expertise in a wide range of photonic materials (from silicon to III-V) and nanotechnologies. He has (co-)authored more than 20 international journal publications and 50 conference papers. He is a member of the IEEE Photonics Society and the Optical Society of America. Currently he serves as a board member of IEEE Photonics Society Benelux Chapter.

Zizheng Cao received the B.S. degree in electronic information science and technology from Hunan Normal University, Changsha, China, the M.E. degree in telecom engineering (awarded outstanding thesis of master's degree of Hunan Province in 2010) from Hunan University, Changsha, China, and the Ph.D. (cum laude) (Hons.) degree from the Eindhoven University of Technology, Eindhoven, The Netherlands, in 2015. Supervised by Prof. T. Koonen, he started his Ph.D. research funded by the NWO Project SOWICI, mainly focusing on energy-efficient access/indoor optical networks empowered by integrated optics, low-complexity digital signal processing (DSP), and flexible optical network design. The research activities produce a series of interesting scientific results. Currently he is working as an assistant professor in Prof. Koonen's group. He has authored 15 first-authored peer-reviewed IEEE/OSA journal articles, including an invited paper in the IEEE JOURNAL OF LIGHTWAVE TECHNOLOGY and an invited paper in IEEE JOURNAL OF QUANTUM ELECTRONICS. He also has an invited talk about integrated optical radio beam steering systems in PIERS2014 and an invited talk about RF-OAM in ACP2015. Currently, his research articles have been cited for 749 times, with H-index of 15 and i10 factor of 23 (source from Google Scholar). He holds two granted Chinese patents and one U.S. provisional patent. His research interests include modeling and design of integrated photonics circuits, microwave photonics, advanced DSP, and physical layer design of optical network. He was a Student Member of the IEEE Photonics Society. He serves as an Active Reviewer of many top IEEE/OSA journals. He was a recipient of the Graduate Student Fellowship of the IEEE Photonics Society 2014.

Longfei Shen was born in Beijing, China, in 1988. He obtained a bachelor degree in Electrical Engineering from the Zhejiang University in 2010. He subsequently moved to Europe to study photonics at the Royal Institute of Technology (KTH), supported by the Erasmus Mundus scholarship. He received his master degree in 2012, with a thesis project performed at Philips Research. In 2016 he received his Ph.D. degree (cum laude) from the Eindhoven University of Technology, based on research in highspeed photodetectors and heterogeneous integration technology. He is now with the JePPIX Technology Center, working on photonics technology development and transfer from academic research to industrial applications.

Jos van der Tol received the M.Sc and Ph.D degrees in physics from the State University of Leiden, The Netherlands in 1979 and 1985, respectively. In 1985 he joined KPN Research, where he became involved in research on integrated optical components for use in telecommunication networks. His research interest in this field have covered modelling of waveguides, design of electro-optical devices on lithium niobate and their fabrication. Furthermore he has been working on guided wave components on III-V semiconductor materials. He has also been active in the field of optical networks, focussing on survivability, introduction scenarios and management issues. Since July 1999 dr. Van der Tol is working as an associate professor at the University of Technology Eindhoven in The Netherlands, where his research interests include opto-electronic integration, polarization issues, photonic membranes and photonic crystals. He is (co-)author of more than 160 Publications in the fields of integrated optics and optical networks, and has 25 patent applications to his name.

Ton Koonen received the degree (cum laude) in electrical engineering from the Eindhoven University of Technology (TU/e), in 1979. He subsequently worked more than 20 years in industrial research (in Philips' Telecommunicatie Industrie, AT&T Network Systems, and in Lucent Bell Laboratories) on high-speed transmission systems and optical fiber

systems for hybrid access networks, from 1987 as a Technical Manager. He was a part-time Professor with Twente University from 1991 to 2000. Since 2001, he has been a fulltime Professor at TU/e, and the Chairman of the Electro-Optical Communication Systems Group at the Department of Electrical Engineering, part of the COBRA Institute, since 2004. Since 2012, he has been the Vice Dean of the Electrical Engineering Department at TU/e, appointed to overlook EE's research activities. In 2014, he was appointed as a Distinguished Guest Professor at Hunan University, Changsha, China. He participated in many projects funded by the European Commission (EC), from the RACE Program up to the FP7 program; amongst others he initiated and led projects in dynamically reconfigurable optical access networks, fiber-wireless networks, and label-controlled optical packet-switched networks in the FP4-FP6 programs. In FP7, he led/leads activities in the projects ALPHA, BONE, POFPLUS, and MODE-GAP. He also started and led a number of nationally funded projects in these fields. He is a Frequent Reviewer of EC projects, and was the Chairman of Panel PE7A for the European Research Council's Advanced Grant Program, and a member of several Dutch R&D Program Committees. His current research interests are in access and in-building fiber network techniques, including multimode fiber networks and radio-over-fiber systems, advanced optical multiplexing schemes (e.g. mode multiplexing), and optical wireless communication. He has (co-)authored more than 650 papers on optical fiber communication, and holds five U.S. patents (+1 pending), and one Dutch patent. He is a Lucent Bell Labs Fellow (1998) and an OSA Fellow (2013). He was also a 2011 recipient of an Advanced Investigator Grant of the European Research Council.